


---

This is the **submitted version** of the journal article:

Guerrero, Miguel; García-Antón, Jordi; Tristany, Mar; [et al.]. «Design of new N,O hybrid pyrazole derived ligands and their use as stabilizers for the synthesis of Pd nanoparticles». Langmuir, Vol. 26, Issue 19 (October 2010), p. 15532-15540. DOI 10.1021/la1016802

---

This version is available at <https://ddd.uab.cat/record/291075>

under the terms of the  <sup>IN</sup> COPYRIGHT license

# Design of new N,O hybrid pyrazole derived ligands and their use as stabilizers for the synthesis of Pd nanoparticles

Miguel Guerrero,<sup>[a,b]</sup> Jordi García-Antón,<sup>[a]\*</sup> Mar Tristany<sup>[b,c]</sup>, Josefina Pons,<sup>[a]</sup> Josep Ros,<sup>[a]</sup> Karine Philippot,<sup>[b,c]\*</sup> Pierre Lecante<sup>[d]</sup> and Bruno Chaudret<sup>[b,c]</sup>.

[a] M. Guerrero, Dr. J. García-Antón, Dr. J. Pons, Dr. J. Ros  
Departament de Química, Unitat de Química Inorgànica, Universitat Autònoma de Barcelona, 08193-Bellaterra, Barcelona, Spain.  
Fax: (+34) 93 581 3101  
E-mail: [Jordi.GarciaAnton@uab.cat](mailto:Jordi.GarciaAnton@uab.cat)

[b] Dr. M. Tristany, Dr. K. Philippot, Dr. B. Chaudret  
CNRS; LCC (Laboratoire de Chimie de Coordination du CNRS), 205, route de Narbonne, F-31077 Toulouse, France  
Fax: (+33) 5 61553003  
E-mail: [Karine.Philippot@lcc-toulouse.fr](mailto:Karine.Philippot@lcc-toulouse.fr)

[c] Université de Toulouse; UPS, INPT ; LCC ; F-31077 Toulouse, France

[d] CNRS, CEMES (Centre d'Elaboration de Matériaux et d'Etudes Structurales), 29 rue J. Marvig, F-31055 Toulouse, France

## Abstract

We describe the stabilization studies of new palladium nanoparticles (Pd NPs) with a family of hybrid ligands. For this purpose, two new *N,O*-hybrid pyrazole derived ligands, as well as other previously reported, have been used as NPs stabilizing agents following an organometallic approach. A comparison with corresponding palladium complexes has been carried out. We have also studied the superstructures formed by the agglomeration of NPs.

In order to evaluate the scope of the system, different parameters have been studied such as the structure of the ligand, the ligand/metal ratio, the nature of the solvent, the concentration and the reaction time. The colloidal materials resulting from the different syntheses were all characterized by IR, transmission electron microscopy techniques at

low or high resolution (TEM and HR-TEM) and scanning electron microscopy (SEM). All these observations have allowed us to better understand the coordination modes of the different ligands onto the surface of the NPs.

## **Introduction**

Colloid materials containing metal nanoparticles have been known for a long time.<sup>1</sup> Current attention on nanotechnology has attracted renewed interest toward metal nanoparticles, from both fundamental and practical points of view, because at a size of particle in the nano range, different physical/chemical properties may occur compared with molecular and bulk metal counterparts. Nowadays, preparation, structural determination, study of the properties and exploration for diverse applications of nanosized particles are hot research topics.<sup>2-6</sup> Moreover, the use of metal nanoparticles for catalytic transformations of organic substrates is a growing area<sup>7-9</sup> and has been recently reviewed.<sup>10-12</sup> Metal nanoparticles have been proved to be efficient and selective catalysts for reactions which are catalyzed by molecular complexes such as olefins hydrogenation or C-C couplings, for example, but also for reactions which are not or poorly catalyzed by molecular species such as arenes hydrogenation.<sup>13,14,15</sup>

Among all transition metals, Pd is probably the most versatile in promoting or catalyzing reactions, many of which are not easily achieved with other transition metals. The success observed using Pd nanoparticles as catalysts has led to a growing demand which in turn has resulted in an exponential growth in the number of nanoparticle synthesis procedures reported for this metal.<sup>16,17</sup> However, the reproducible preparation of small and stable palladium nanoparticles with a narrow size distribution is of high importance and still remains a challenging task. Unfortunately, as the size of the nanoparticle gets smaller, the preparation becomes more laborious because of their high

tendency to aggregate. For this reason, a major demand exists in the ability to produce well-defined and monodisperse Pd nanoparticles in the 1-4 nm size range. Pd nanoparticles have been prepared by methods like inverse micelle systems,<sup>18,19</sup> reduction of palladium acetate,<sup>20</sup> electrochemical synthesis,<sup>21</sup> reduction of palladium salts<sup>22,23</sup> or sonochemical reduction.<sup>24</sup>

The decomposition of organometallic precursors under mild conditions represents an alternative synthetic methodology to give well-controlled metallic nanoparticles displaying a very small size.<sup>25,26</sup> This characteristic is a key aspect for their subsequent applications in catalysis where a high surface atom number will favor a higher activity.<sup>27</sup> Nevertheless, the presence of a stabilizing agent is required to prevent the facile agglomeration of the particles and the precipitation of “palladium black”. As a result, besides the synthesis methodology, the stabilizer is also a key-point in nanoparticles synthesis. In the literature, several kinds of stabilizers such as dendrimers,<sup>28-30</sup> polymers<sup>31-33</sup> or surfactants<sup>34,35</sup> have been reported. Recently, the use of coordinating ligands like phosphines,<sup>36-38</sup> thiols,<sup>39,40</sup> thioethers,<sup>41</sup> or amines<sup>42-44</sup> has been developed. But most of the time, commercial or simple ligands are used and the resulting catalytic properties show that they are not well adapted to the surface of metal nanoparticles since they do not lead to efficient catalytic properties, more particularly in asymmetric catalysis. Nevertheless, recent findings show that more sophisticated ligands can modify the reactivity of small nanoparticles in a way similar to the orientation of reactivity achieved by ligands in molecular organometallic complexes.<sup>45</sup> It is thus necessary to design ligands to act as efficient stabilizers for metal nanoparticles without loss of their reactivity. For that purpose, the development of new hybrid ligands (also called mixed ligands) containing two or more differentiated donor moieties, represents an interesting alternative. Such ligands will chemically coordinate

on the particle surface and protect them from aggregation. To improve the design of ligands well-adapted to the surface of metal nanoparticles, it is very important to understand the role of each functional group of the ligand in the stabilization of metal particles but, unfortunately, this is not always possible. Even if the coordination chemistry of the ligands may be different in the molecular complexes and onto the surface of the NPs, the study of the behavior of these ligands in metal complexes can provide valuable information about their coordination abilities.

In this paper we report a family of ligands, namely N,O hybrid bis or tris-pyrazole ligands (**L1-L6**), which have been used as stabilizing agents for the synthesis of palladium nanoparticles through an organometallic methodology. Taking into account previous results,<sup>46,47</sup> these ligands appeared to us interesting since they have different sites for anchorage at the particle surface: 1) the pyrazole rings can interact with the metal surface through nitrogen donor atoms or through  $\pi$ -interaction; 2) the oxygen atom of the alkylether chain may complete the ligand coordination; and 3) the introduction of phenyl rings may also complete the coordination of the ligand by  $\pi$ -interaction. We have also tested 1-(2-hydroxyethyl)-3,5-dimethylpyrazole ligand (**L0**, precursor of **L2-L6**), in order to compare the effect between mono-, bis- and tris-pyrazolyl ligands.

## Results

### 1. Synthesis of alkylether N-substituted pyrazole ligands

The following alkylether N-substituted pyrazole ligands (Scheme 1) have been synthesized: 1,8-bis(3,5-dimethyl-1*H*-pyrazol-1-yl)-3,6-dioxaoctane (**L1**), 1,2-bis[4-(3,5-dimethyl-1*H*-pyrazol-1-yl)-2-oxabutyl]benzene (**L2**), 1,3-bis[4-(3,5-dimethyl-1*H*-pyrazol-1-yl)-2-oxabutyl]benzene (**L3**), 1,4-bis[4-(3,5-dimethyl-1*H*-pyrazol-1-yl)-2-

oxabutyl]benzene (**L4**), 4,4'-bis[4-(3,5-dimethyl-*1H*-pyrazol-1-yl)-2-oxabutyl]biphenyl (**L5**) and 1,3,5-tris[4-(3,5-dimethyl-*1H*-pyrazol-1-yl)-2-oxabutyl]benzene (**L6**).

Compounds **L5** and **L6** were synthesized for the first time in this work, using a similar reaction pathway published for **L1-L4**.<sup>48,49</sup> The synthetic procedure for **L5** and **L6** consists of two steps (Scheme 2). Firstly, 1-(2-hydroxyethyl)-3,5-dimethylpyrazole<sup>50,51</sup> was reacted with NaH in dry tetrahydrofuran to give the corresponding sodium alkoxide. In the second step, this sodium salt was converted to the corresponding ligand (**L5** or **L6**) by reaction with the appropriate reagent (**L5** = 0.50 equivalents of 4,4'-bis(chloromethyl)-1,1'-biphenyl; **L6** = 0.33 equivalents of 1,3,5-tris(bromomethyl)benzene) in dry tetrahydrofuran.

All the ligands have been fully characterized by determination of their melting point, elemental analysis, mass spectrometry, IR and <sup>1</sup>H and <sup>13</sup>C{<sup>1</sup>H} NMR spectroscopies. The NMR signals were assigned by reference to the literature<sup>52,53</sup> and from DEPT, COSY and HMQC NMR experiments. Elemental analyses, mass spectrometry and all spectroscopic data for **L5** and **L6** are consistent with the proposed structures.

## **2. Synthesis of Pd nanoparticles in the presence of alkylether N-substituted pyrazole ligands**

**L1-L6** ligands have been used as stabilizing agents of nanosized Pd particles. These particles have been prepared according to the organometallic method developed by some of us (Scheme 3).<sup>54</sup> The organometallic complex [Pd<sub>2</sub>(dba)<sub>3</sub>] (dba = dibenzylideneacetone) was used as Pd source. The syntheses of the nanoparticles were carried out in a Fisher-Porter reactor under 3 bar of dihydrogen, at room temperature and in the presence of the chosen ligand among **L1-L6**. In order to determine the influence of reaction conditions on the mean size of the nanoparticles, several

parameters were evaluated, namely: nature of ligand (**L1-L6**), ligand/metal ratio ( $[L]/[Pd]$ ), nature of solvent (a coordinating one as THF or a non-coordinating one as toluene), reaction time (1, 5 or 20 hours) and concentration of the reagents. Experimental data of the synthesis of the nanoparticles are reported in Table 1 and details are described in the experimental section. The colloidal materials resulting from the different syntheses were all characterized by transmission electron microscopy techniques at low or high resolution (TEM and HR-TEM). Representative images of the resulting Pd nanoparticles (Pd NPs) are given in Figure 1. Moreover, the IR spectra of the NPs in the range 4000-400  $\text{cm}^{-1}$  show that the ligands **L1-L6** are not altered during NPs synthesis and that they are coordinated onto the surface of the NPs.

$^1\text{H}$  and DOSY NMR studies with several samples of Pd NPs have been carried out. Unfortunately, these experiments did not give rise to conclusive results as the NPs are not very soluble in THF- $d_8$  or in other deuterated solvents.

During the synthesis of Pd NPs, we observed that all the tested ligands except **L6** need to be added in the reaction medium with a  $[L]/[Pd]$  ratio of at least 0.2 to stabilize efficiently the particles. If the  $[L1-L5]/[Pd]$  ratio is lower (for example 0.1) black metal powders containing large and dense aggregates of nanoparticles are formed, while **L6** is capable of stabilizing well separated small particles in these conditions (Table 1, entry 27, Figure 1f). The use of a higher  $[L]/[Pd]$  ratio was thus investigated and is hereafter commented for each ligand.

With **L1**, the mean size of the obtained Pd NPs, *ca.* 4.2 nm, does not significantly depend on the  $[L]/[Pd]$  ratio, (see Figure 2, Table 1, entries 4-6). More or less spherical superstructures containing individual nanoparticles are obtained and they are irregular in size (Figures 1a and 3a).

On the contrary, with **L2**, the mean size of Pd NPs varies with the  $[L]/[Pd]$  ratio from 4.2 nm (0.2 eq.) to 2.5 nm (1.0 eq.) (Table 1, entries 8, 10 and 11, Figure 1b), the size of the Pd NPs significantly decreasing with increasing quantity of **L2** (Figure 2). Superstructures are also obtained with this ligand, which are also irregular in size. These superstructures are larger than those obtained with **L1**, and their size tends to decrease when the concentration of the reagents in the reaction medium decreases (Table 1, entries 8 and 9, Figures 1b and 3b).

**L3** (Table 1, entries 13, 14) and **L4** (Table 1, entries 15-17) did not lead to satisfactory results regarding the stabilization of Pd NPs (formation of precipitates) except when a  $[L4]/[Pd]$  ratio of 1.0 was used. In this case, Pd NPs with a mean size of *ca.* 4.4 nm are formed that are embedded into irregular superstructures (Table 1, entry 17, Figure 1c).

The structure of **L4** ligand probably induces its coordination to the NPs metal surface via only one of the pyrazolyl rings (Scheme 4a). In order to check the effect of the steric hindrance provoked by the free pyrazole-ether chain, we synthesized a new hybrid ligand similar to **L4** but containing a biphenyl ring instead of a simple phenyl ring (**L5**, Scheme 1). In this case, and in contrast to what we have previously observed with **L4**, a  $[L5]/[Pd]$  ratio of 0.2 was enough to get stable Pd NPs with a mean size of *ca.* 2.7 nm (Table 1, entry 19, Figure 3c). However, we did not notice a significant variation of the particles mean size for higher  $[L5]/[Pd]$  ratio, as previously observed with **L1** (Figure 2). Nevertheless, the colloids obtained with  $[L5]/[Pd] = 0.2$  (Table 1, entry 19; 2.7 nm) are smaller than with  $[L1]/[Pd] = 0.2$  (Table 1, entry 4, 4.2 nm).

It is also interesting to note the effect of ligand **L5** in the formation of superstructures resulting from assembly of Pd NPs (Figures 3c and 3d). When a small amount of ligand is used ( $[L5]/[Pd]$  ratio=0.2), spherical assemblies of *ca.* 120 nm, more or less regular in size and containing small Pd NPs are observed (Table 1, entry 19, Figure 3c). In the



presence of a large amount of **L5** (5.0 eq.), the nanoparticles appear separated on the microscopy grid, embedded in the matrix of ligand (Table 1, entry 26, Figures 1e and 3d). The difference observed between these two samples is more evident on the SEM-FEG images where a continuous layer of nanoparticles is observed for 5 eq. of **L5** (Figure 4). It is also important to note that there is a good correlation in the mean size of the spherical assemblies when obtained from TEM or SEM-FEG images. For example, the mean size of the spherical assemblies obtained with  $[\text{L5}]/[\text{Pd}]=0.2$  is 120(10) nm for TEM and 118(15) nm for SEM-FEG. Additionally, in order to obtain the size of the aggregates in solution, we have carried out selected Dynamic Light Scattering (DLS) experiments (Figures S1 and S2, Supporting Information). In particular, measurements of  $[\text{L2}]/[\text{Pd}] = 0.5$  (168 nm) and  $[\text{L5}]/[\text{Pd}] = 0.2$  (124 nm) are in agreement with the TEM / SEM-FEG data mentioned above.

In order to circumvent the lack of stabilization observed with **L3**, we have designed a new ligand, **L6**. This new ligand is very similar to **L3**, but it displays a tripodal structure, since a new alkylpyrazole-ether chain has been grafted in the 5-relative position of the phenyl ring (Scheme 1). In comparison with **L3**, this new ligand **L6** gave rise to stable colloidal solutions (Figures 3e and 3f), while **L3** led only to precipitates. A comparison between **L6** and **L4** points out that **L6** is a better stabilizer since at least a ratio  $[\text{L4}]/[\text{Pd}]=1.0$  is necessary to obtain stable colloidal solutions while a  $[\text{L6}]/[\text{Pd}]$  ratio of 0.1 is enough (Table 1, entry 27, Figure 1f). Finally, if we compare the effect of **L6** on the mean size of the particles with that of **L2**, we can conclude that they present a similar behavior. Indeed, with **L6** we obtained Pd NPs with a mean size of *ca.* 4.0 ( $[\text{L6}]/[\text{Pd}]$  ratio=0.2) to *ca.* 2.6 nm ( $[\text{L6}]/[\text{Pd}]$  ratio=1.0) (Table 1, entries 28 and 30) against *ca.* 4.2 ( $[\text{L2}]/[\text{Pd}]$  ratio=0.2) and *ca.* 2.5 ( $[\text{L2}]/[\text{Pd}]$  ratio=1.0) with **L2** (Table 1, entries 8 and 11). This shows, in comparison with **L3**, that the introduction of a third

alkylpyrazole-ether chain highly improves the stabilization of the colloids giving rise to Pd NPs with a mean size decreasing with a ligand increase (Figure 2).

Wide-Angle X-Rays Scattering (WAXS) measurements have been performed on a few isolated samples, namely samples obtained for [L2]/[Pd]=0.5 (Table 1, entry 10), [L5]/[Pd]=0.2 (Table 1, entry 19) and [L6]/[Pd]=0.2 (Table 1, entry 28). These Pd NPs clearly adopt the crystalline structure of bulk palladium (Figure 5a). All the related Radial Distribution Functions (RDF, Figure 5b) are very similar in shape, amplitude and extent, and also quite similar to the function computed from a 3.5 nm fcc model based on bulk Pd. These Pd NPs clearly adopt the crystalline structure of bulk palladium. From the dampening of the RDFs, the average size of the crystalline domains can be estimated in the 3.5-4.0 nm range, not significantly different from the sizes obtained from TEM (3.1, 2.7 and 4.0 nm, respectively), clearly indicating that the NPs are single crystals. Electron diffraction (ED) confirms the presence of face centered cubic (fcc) palladium(0) in all the samples. Figure 6 shows the interplanar spacing of (111) Pd planes (2.24 Å).

### **3. Synthesis of Pd complexes in the presence of alkylether N-substituted pyrazole ligands**

Although the coordination of a ligand on an isolated Pd atom in a molecular complex is probably a little different from that on a particle surface, we thought that the behavior of the ligand in complexes could shed some light on our study. For that purpose, we prepared Pd molecular complexes with the same pyrazole ligands. This allowed us to know their preferential coordination mode and further, to better understand the coordination ability of these ligands at the particle surface and the potential influence of this coordination on the stabilization and the control of the size of Pd NPs.

The coordination chemistry of **L1-L4** ligands towards Pd(II) has been recently described in the literature.<sup>48,49</sup> Monomeric  $[\text{PdCl}_2(\text{L})]$  and dimeric  $[\text{PdCl}_2(\text{L})]_2$  complexes have been obtained depending on the solvent and conditions of the reaction: when **L1-L6** ligands react with  $[\text{PdCl}_2(\text{CH}_3\text{CN})_2]$  in acetonitrile they yield monomers while dimers are formed when THF is used (Scheme 5). We have observed that the N,O hybrid ligands coordinate to the metal centers via the N of the pyrazole rings, whereas the ether moieties remain uncoordinated.

## Discussion

Taking into account the obtained results in coordination chemistry with Pd(II), we consider that N,O hybrid pyrazole ligands only coordinate through the nitrogen atoms as these are better coordinating donor atoms than the ether moieties. Indeed, we have only observed this type of coordination in the crystal structure of the molecular Pd(II) complexes (**1A**, **2A** and **2B**) (Scheme 5).<sup>48,49</sup> This hypothesis is further used to compare the coordination of the ligands at the particles surface.

In addition to the tests performed with the ligands, the 1-(2-hydroxyethyl)-3,5-dimethylpyrazole (**L0**), precursor of **L2-L6** ligands, has also been tested as a stabilizing agent in the synthesis of Pd nanoparticles using  $[\text{L0}]/[\text{Pd}]=0.1-5.0$ . With this ligand, the decomposition of  $[\text{Pd}_2(\text{dba})_3]$  led to the precipitation of Pd as a black powder even when a large quantity of ligand (5 eq.) was used (Table 1, entry 2). These experiments suggest that the coordination of the pyrazolyl groups on the nanoparticles is weak and that the ligands are labile on the surface. This further suggests that at least two pyrazolyl groups are necessary to stabilize the particles thanks to a chelating effect, i.e. a kinetic effect.

In the case of **L1**, we observed the formation of Pd NPs with a mean size of *ca.* 4.2 nm whatever the quantity of added ligand, with a slight tendency to self-assembly (Figure

1a). This suggests a very weak coordination of the ligand, probably through only one nitrogen group and a very fluxional system.

In contrast to what we found for **L1**, **L2** gave rise to a significant variation of the mean size of the nanoparticles depending on the  $[\mathbf{L2}]/[\text{Pd}]$  ratio, with a decreasing size when this ratio increases. This suggests that **L2** is indeed coordinated on the particles with enough strength to influence their growth process. This can result from the presence of the two pyrazolyl moieties in *ortho* position which can serve as a pincer as well as from the presence of a phenyl ring which may coordinate flat on the particles<sup>46</sup> (Scheme 4b). The presence of an equilibrium is attested by the influence of the concentration of **L2** on the size of the particles which is an indication of the number of ligands coordinated at the particles surface. DOSY NMR experiments, despite the low quality of the spectra due to a lack of solubility of the particles, seem to corroborate that **L2** is not strongly attached at the particle surface.

The pincer hypothesis is supported by the differences found in **L1** and **L2** coordination in the molecular Pd(II) complex  $[\text{PdCl}_2(\mathbf{L})]$  (**1A** and **2A**, Scheme 5). Complex **2A** presents a higher distortion on the square-planar geometry than **1A** showing the less flexibility of **L2**.<sup>48,49</sup> As happened with **L1**, we have also obtained spherical superstructures with **L2** (Figure 3b) which result from the lack of spatial extension of the ligands.

The unsatisfactory results obtained with **L3**, which contains a phenyl ring substituted in *meta* position, may be explained by its intermediate coordination mode on the surface of the nanoparticles. No pincer type coordination is expected with this ligand and the *meta* position of the substituents is unfavorable for a  $\pi$ -coordination. The newly synthesized tripodal ligand **L6**, obtained by adding a new alkylpyrazole chain in the 5-relative position of the phenyl ring (Scheme 1), corrects this disadvantage. Even if this ligand

still coordinates at the particle surface in the same manner as **L3** (*via* two N pyrazolyl rings), **L6** has a third alkylpyrazole chain that can complete the ligand coordination through a chelating effect extended to three weakly coordinating groups. It may also induce the necessary steric hindrance around the particles to avoid their agglomeration (Scheme 4c).

In opposition with the behavior of *ortho* (**L2**) and *meta* (**L3**) ligands and similarly to **L1**, **L4** can coordinate to nanoparticle surface via only one of its pyrazolyl groups (Scheme 4a), due to the *para* relative substitution of the two alkylpyrazolyl chains in the phenyl ring. In this case, a ligand concentration  $[\text{L4}]/[\text{Pd}]=1.0$  was needed to obtain some stabilization of the Pd NPs.

The use of **L5** which contains a biphenyl ring, results in an improvement of the nanoparticles stabilization. In this case, we always obtain nanoparticles of *ca.* 2.7 nm for  $[\text{L5}]/[\text{Pd}] \geq 0.2$  (Table 1, entries 19-25). Spherical superstructures containing individual Pd NPs are also observed when the quantity of ligand is low (Figure 3c). For a large ligand excess ( $[\text{L5}]/[\text{Pd}]=5.0$ ), spherical assemblies are no longer obtained but a continuous layer of nanoparticles is formed showing that Pd NPs are close together (Figure 3d). This suggests first a strong interaction between **L5** and the particles surface. This may be due to the presence of the biphenyl moieties able to strongly interact with the palladium surface. The small size of the particles obtained in this case and the absence of size variation as a function of the ligand concentration points to this strong coordination of **L5**. The particles display little interaction between them; the aggregation observed at low ligand concentration can be disrupted at high ligand coverage, either thanks to coordination of excess **L5** through one pyrazolyl group or to supramolecular interactions.

DOSY NMR experiments suggest that **L5** and **L6** ligands are more strongly attached at the NPs surface but their poor quality, as result of the lack of solubility, prevents any quantitative or at least more conclusive comment.

In addition, we have carried out some complementary experiments to examine the scope of the present stabilizing agents. As an example, with **L5** ( $[\text{L5}]/[\text{Pd}]=0.2$ ) we observed that the reaction time does not affect the size and the morphology of the nanoparticles and superstructures (Table 1, entries 19 (20h), 22 (1h), 23 (5h)). Similarly, we did not observe significant difference by changing THF for toluene as the solvent of the reaction, (Table 1, entries 19 (THF) and 21 (toluene)). With the system **L2** ( $[\text{L2}]/[\text{Pd}]=1.0$ ), the use of toluene or THF did not affect the synthesis of the nanoparticles (Table 1, entries 11 and 12). Finally, when the initial concentration of the reagents in the  $[\text{L5}]/[\text{Pd}]=0.2$  system was diluted, we did not either notice any significant difference in the mean size of the NPs and superstructures (Table 1, entry 19 and 20). However, we observed that for the  $[\text{L2}]/[\text{Pd}]=0.2$  system, there were some differences in the mean size of the spherical assemblies: 130 nm (entry 8, 1 mg Pd precursor/mL) and 40 nm (entry 9, 0.5 mg Pd precursor/mL).

## Conclusion

In summary, the synthesis of Pd nanoparticles in the presence of N,O hybrid pyrazole ligands was successfully carried out. A comparison of the results of these syntheses with those obtained with the corresponding Pd complexes allowed us to get information on the coordination ability of such ligands at the particle surface. It is therefore possible to conclude that the pyrazolyl groups are weak ligands and consequently that at least two of them are necessary to stabilize Pd NPs efficiently. When two pyrazolyl groups are present in the ligand, their position relative to a phenyl group may be a key-factor to

orientate their coordination mode at the particle surface and thus the Pd NPs stabilization.

While the *ortho* ligand (**L2**) favors the coordination of both pyrazolyl moieties to one single nanoparticle, *meta* (**L3**) and *para* (**L4**) ligands are not good for the NPs stabilization. New designed and synthesized ligands (**L5** and **L6**) improve these results and provoke the link between nanoparticles by the means of the different pyrazolyl rings. In the case of **L5**, which appears to be the best ligand to obtain smaller nanoparticles, the presence of two arene rings capable of  $\pi$ -coordinating on the surface of the particles may be the critical point. As previously observed, the conjunction of weak nitrogen ligands able to kinetically approach the nanoparticle with phenyl rings able to strongly coordinate on the particle surface may be a key point to prepare new ligands fully adapted to nanoparticles. It is noteworthy that this is the type of structure adopted by cinchonidine which remains the best substituent for achieving catalytic asymmetric reactions on nanoparticles.

## Experimental Section

### 1. General procedure and reagents

All manipulations were carried out under argon atmosphere using standard Schlenk tube or Fischer–Porter reactor and vacuum line techniques, or in a glove-box.  $[\text{Pd}_2(\text{dba})_3]$  was purchased from Strem Chemicals and  $[\text{PdCl}_2(\text{CH}_3\text{CN})_2]$  was prepared as described in the literature<sup>55</sup>. **L1**<sup>49</sup> and **L2-L4**<sup>48</sup> ligands were synthesized following methodologies previously described. Solvents were purchased from SDS and dried through a purification machine (MBraun MB SPS-800) or distilled prior to use: THF over sodium/benzophenone, toluene over sodium and pentane over calcium hydride.

Melting points were measured on an Electrothermal 1A8104 melting point apparatus. Elemental analyses (C, H, and N) were carried out by the staff of Chemical Analyses Service of the Universitat Autònoma de Barcelona on a Eurovector 3011 instrument. Infrared spectra were run on a Perkin Elmer FT spectrophotometer, series 2000  $\text{cm}^{-1}$  as KBr pellets or polyethylene films in the range 4000-150  $\text{cm}^{-1}$ .  $^1\text{H}$  NMR,  $^{13}\text{C}$   $\{^1\text{H}\}$  NMR, HSQC, COSY and NOESY spectra were recorded on a Bruker AVANCE 250 MHz NMR spectrometer in  $\text{CDCl}_3$  solutions at room temperature. All chemical shifts values ( $\delta$ ) are given in ppm. Electrospray mass spectra were obtained with an Esquire 3000 ion trap mass spectrometer from Bruker Daltonics.

Specimens for TEM/HR-TEM and SEM-FEG analyses were prepared by slow evaporation of a drop of crude colloidal solution deposited under argon onto holey carbon-covered copper grids. In some cases grids were prepared after dispersion in THF of the isolated nanomaterial after precipitation with pentane. TEM/HR-TEM and SEM analyses were performed at “Servei Microscopia de la UAB” with a JEOL JEM 2010 electron microscope working at 200 kV with a resolution point of a 2.5 Å and with a HITACHI S-570 electron microscope working at 15 kV and at 2 mm WD, respectively. The size distributions were determined via manual analysis of enlarged micrographs by measuring *ca.* 200 particles on a given grid to obtain a statistical size distribution and a mean diameter.

Data collection for WAXS was performed at the CEMES-CNRS (Toulouse) on small amounts of powder. All samples were sealed in 1 mm diameter Lindemann glass capillaries. The measurements of the X-ray intensity scattered by the samples irradiated with graphite monochromatized  $\text{MoK}\alpha$  (0.071069 nm) radiation were performed using a dedicated two-axis diffractometer. Measurement time was 15h for each sample. Scattering data were corrected for polarization and absorption effects, then normalized



to one Pd atom and Fourier transformed to obtain the RDFs. To make comparisons with the crystalline structure in real space, a model was generated from bulk Pd parameters. The classic Debye's function was then used to compute intensity values subsequently Fourier transformed in the same conditions than the experimental ones.

## 2. Synthesis and characterization of Ligands L5 and L6.

A solution of 4.20 g (0.030 mol) of 1-(2-hydroxyethyl)-3,5-dimethylpyrazole<sup>50,51</sup> in 50 mL of tetrahydrofuran was slowly added to a suspension of 0.80 g (0.033 mol) of NaH in 20 mL of tetrahydrofuran. The solution was stirred at 60 °C for 2 h. A total of 3.77 g (0.015 mol) of 4,4'-bis(chloromethyl)-1,1'-biphenyl for **L5** or 3.57 g (0.010 mol) of 1,3,5-tris(bromomethyl)benzene for **L6** in 20 mL of tetrahydrofuran was added dropwise and under vigorous stirring. The resulting mixture was allowed to stir for 12 h at 60 °C. After cooling to room temperature, 10 mL of water was added dropwise to destroy excess NaH. The solvents were then evaporated under reduced pressure. The residue was taken up in water (40 mL) and extracted with chloroform (3-50 mL). The chloroform layers were dried with anhydrous MgSO<sub>4</sub> and evaporated.

**Ligand L5.** Yield: 83% (5.71 g). m.p. 55.2-56.4 °C. C<sub>28</sub>H<sub>34</sub>N<sub>4</sub>O<sub>2</sub>: Anal. Calcd. for C<sub>28</sub>H<sub>34</sub>N<sub>4</sub>O<sub>2</sub>: C, 73.33; H, 7.47; N, 12.22. Found: C, 73.15; H, 7.57; N, 12.01. MS *m/z* (%) = 481.3 (100%) [L+Na]<sup>+</sup>. IR (KBr, cm<sup>-1</sup>): 3070 [ν(C-H)<sub>ar</sub>], 2950, 2865 [ν(C-H)<sub>al</sub>], 1548 [(ν(C=C), ν(C=N))<sub>ar</sub>], 1454 [(δ(C=C), δ(C=N))<sub>ar</sub>], 1107 [ν(C-O-C)], 808 δ(C-H)<sub>oop</sub>. <sup>1</sup>H NMR (CDCl<sub>3</sub> solution, 250 MHz) δ: 7.53 (d, 4H, Ph), 7.29 (d, 4H, Ph), 5.79 (s, 2H, CH(pz)), 4.48 (s, 4H, OCH<sub>2</sub>Ph), 4.17 (t, 4H, <sup>3</sup>J = 5.6 Hz, N<sub>pz</sub>CH<sub>2</sub>CH<sub>2</sub>O), 3.83 (t, 4H, <sup>3</sup>J = 5.6 Hz, N<sub>pz</sub>CH<sub>2</sub>CH<sub>2</sub>O), 2.26 (s, 6H, CH<sub>3</sub>(pz)), 2.23 (s, 6H, CH<sub>3</sub>(pz)) ppm. <sup>13</sup>C{<sup>1</sup>H} NMR (CDCl<sub>3</sub> solution, 63 MHz,) δ: 147.7 (pz-C), 139.9 (pz-C), 137.5-127.1

(Ph), 104.9 (CH(pz)), 72.9 (OCH<sub>2</sub>Ph), 69.4 (N<sub>pz</sub>CH<sub>2</sub>CH<sub>2</sub>O), 48.7 (N<sub>pz</sub>CH<sub>2</sub>CH<sub>2</sub>O), 13.6 (CH<sub>3</sub>(pz)), 11.2 (CH<sub>3</sub>(pz)) ppm.

**Ligand L6.** Yield: 78% (4.17 g). m.p. 44.3-45.3 °C. C<sub>30</sub>H<sub>42</sub>N<sub>6</sub>O<sub>3</sub>: Anal. Calcd. for C<sub>30</sub>H<sub>42</sub>N<sub>6</sub>O<sub>3</sub>: C, 67.39; H, 7.92; N, 15.72. Found: C, 67.45; H, 8.18; N, 15.70. MS *m/z* (%) = 557.3 (100%) [L+Na]<sup>+</sup>. IR (KBr, cm<sup>-1</sup>): 3101 [ν(C-H)<sub>ar</sub>], 2923, 2856 [ν(C-H)<sub>al</sub>], 1552 [(ν(C=C), ν(C=N))<sub>ar</sub>], 1459 [(δ(C=C), δ(C=N))<sub>ar</sub>], 1108 [ν(C-O-C)], 774 [δ(C-H)<sub>oop</sub>]. <sup>1</sup>H NMR (CDCl<sub>3</sub> solution, 250 MHz) δ: 6.96 (s, 3H, Ph), 5.75 (s, 3H, CH(pz)), 4.37 (s, 6H, OCH<sub>2</sub>Ph), 4.13 (t, 6H, <sup>3</sup>J = 4.9 Hz, N<sub>pz</sub>CH<sub>2</sub>CH<sub>2</sub>O), 3.76 (t, 4H, <sup>3</sup>J = 4.9 Hz, N<sub>pz</sub>CH<sub>2</sub>CH<sub>2</sub>O), 2.21 (s, 9H, CH<sub>3</sub>(pz)), 2.19 (s, 9H, CH<sub>3</sub>(pz)) ppm. <sup>13</sup>C{<sup>1</sup>H} NMR (CDCl<sub>3</sub> solution, 63 MHz) δ: 147.5 (pz-C), 139.7 (pz-C), 139.4-125.6 (Ph), 104.7 (CH(pz)), 72.8 (OCH<sub>2</sub>Ph), 69.3 (N<sub>pz</sub>CH<sub>2</sub>CH<sub>2</sub>O), 48.4 (N<sub>pz</sub>CH<sub>2</sub>CH<sub>2</sub>O), 14.0 (CH<sub>3</sub>(pz)), 11.0 (CH<sub>3</sub>(pz)) ppm.

### 3. Synthesis and characterization of Complexes [PdCl<sub>2</sub>(L)] (L = L5 (5A); L = L6 (6A)) and [PdCl<sub>2</sub>(L)]<sub>2</sub> (L = L5 (5B); L = L6 (6B)).

#### 3.1 Synthesis of Complexes [PdCl<sub>2</sub>(L5)] (5A) and [PdCl<sub>2</sub>(L5)]<sub>2</sub> (5B).

A CH<sub>3</sub>CN solution (20 ml) for **5A** or a THF solution (20 ml) for **5B** of [PdCl<sub>2</sub>(CH<sub>3</sub>CN)<sub>2</sub>] (70 mg, 0.270 mmol) was added to a CH<sub>3</sub>CN solution (5 ml) (**5A**) or to a THF solution (5 ml) (**5B**) of the **L5** ligand (0.124 g, 0.270 mmol), and the resulting solution was allowed to stir for 216 h at 60°C (**5A**) or 12 h at room temperature (**5B**). The solvent was removed in vacuo to yield a yellow solid, which was filtered off, washed with 10 ml of diethyl ether and dried in vacuum.

**5A.** Yield: 41% (0.071 g). Anal. Calcd. for  $C_{28}H_{34}Cl_2N_4O_2Pd$ : C, 52.88; H, 5.39; N, 8.81. Found: C, 52.65; H, 5.31; N, 8.92. Conductivity ( $S\ cm^2\ mol^{-1}$ ,  $1.14\ 10^{-3}\ M$  in  $CH_3CN$ ): 31.8. MS  $m/z$  (%) = 658.9 (100%)  $[M+Na]^+$ . IR (KBr,  $cm^{-1}$ ): 3120  $[v(C-H)_{ar}]$ , 2919, 2856  $[v(C-H)_{al}]$ , 1557  $[(v(C=C), v(C=N))_{ar}]$ , 1422  $[(\delta(C=C), \delta(C=N))_{ar}]$ , 1102  $[v(C-O-C)]$ , 799  $[\delta(C-H)_{oop}]$ . (Polyethylene,  $cm^{-1}$ ): 495  $[v(Pd-N)]$ , 349  $[v(Pd-Cl)]$ .  $^1H$  NMR ( $CDCl_3$  solution, 250 MHz)  $\delta$ : 7.33 (dd, 8H, Ph), 5.88 (s, 2H,  $CH(pz)$ ), 4.92 (t, 4H,  $^3J = 6.9\ Hz$ ,  $N_{pz}CH_2CH_2O$ ), 4.40 (s, 4H,  $OCH_2Ph$ ), 4.30 (t, 4H,  $^3J = 6.9\ Hz$ ,  $N_{pz}CH_2CH_2O$ ), 2.87 (s, 6H,  $CH_3(pz)$ ), 2.30 (s, 6H,  $CH_3(pz)$ ) ppm.  $^{13}C\{^1H\}$  NMR ( $CDCl_3$  solution, 63 MHz)  $\delta$ : 150.3 (pz-C), 144.4 (pz-C), 140.1-127.1 (Ph), 107.7 ( $CH(pz)$ ), 73.4 ( $OCH_2Ph$ ), 68.9 ( $N_{pz}CH_2CH_2O$ ), 49.9 ( $N_{pz}CH_2CH_2O$ ), 15.2 ( $CH_3(pz)$ ), 12.3 ( $CH_3(pz)$ ) ppm.

**5B.** Yield: 77% (0.132 g).  $C_{56}H_{68}Cl_4N_8O_4Pd_2$ : Anal. Calc.: C, 52.88; H, 5.39; N, 8.81; Found: C, 53.01; H, 5.23; N, 8.89. Conductivity ( $S\ cm^2\ mol^{-1}$ ,  $1.02\ 10^{-3}\ M$  in  $CH_3CN$ ): 43.2. MS ( $m/z$ ) (%) = 1237.1 (100%)  $[M-Cl]^+$ . IR (KBr,  $cm^{-1}$ ): 3120  $v(C-H)_{ar}$ , 2921, 2859  $v(C-H)_{al}$ , 1556  $(v(C=C), v(C=N))_{ar}$ , 1400  $(\delta(C=C), \delta(C=N))_{ar}$ , 1104  $v(C-O-C)_{as}$ , 804  $\delta(C-H)_{oop}$ . (Polyethylene,  $cm^{-1}$ ): 479  $v(Pd-N)$ , 362  $v(Pd-Cl)$ .  $^1H$  NMR ( $CDCl_3$  solution, 250 MHz)  $\delta$ : 7.53 (m, 8H, Ph), 5.89 (m, 2H,  $CH(pz)$ ), 5.05 (m, 4H,  $N_{pz}CH_2CH_2O$ ), 4.48 (m, 4H,  $OCH_2Ph$ ), 4.41 (m, 4H,  $N_{pz}CH_2CH_2O$ ), 2.90 (m, 6H,  $CH_3(pz)$ ), 2.31 (m, 6H,  $CH_3(pz)$ ) ppm.  $^{13}C\{^1H\}$  NMR ( $CDCl_3$  solution, 63 MHz)  $\delta$ : 150.4 (pz-C), 144.4 (pz-C), 137.2-127.2 (Ph), 107.7 ( $CH(pz)$ ), 73.3 ( $OCH_2Ph$ ), 68.9 ( $N_{pz}CH_2CH_2O$ ), 49.9 ( $N_{pz}CH_2CH_2O$ ), 15.2 ( $CH_3(pz)$ ), 12.2 ( $CH_3(pz)$ ) ppm.

4.2 Synthesis of Complexes  $[PdCl_2(L6)]$  (**6A**) and  $[PdCl_2(L6)]_2$  (**6B**).

A CH<sub>3</sub>CN solution (20 ml) for **6A** or a THF solution (20 ml) for **6B** of [PdCl<sub>2</sub>(CH<sub>3</sub>CN)<sub>2</sub>] (70 mg, 0.270 mmol) was added to a CH<sub>3</sub>CN solution (5 ml) (**6A**) or to a THF solution (5 ml) (**6B**) of the **L6** ligand (0.144 g, 0.270 mmol), and the resulting solution was allowed to stir for 72 h at 60°C (**6A**) or 12 h at room temperature (**6B**). The solvent was removed in vacuo to yield a yellow solid, which was filtered off, washed with 15 ml of diethyl ether and dried in vacuum.

**6A.** Yield: 56% (0.107 g). C<sub>30</sub>H<sub>42</sub>Cl<sub>2</sub>N<sub>6</sub>O<sub>3</sub>Pd: Anal. Calc.: C, 50.61; H, 5.95; N, 11.80; Found: C, 50.32; H, 5.76; N, 11.75. Conductivity (S cm<sup>2</sup> mol<sup>-1</sup>, 1.08 10<sup>-3</sup> M in CH<sub>3</sub>CN): 18.1. MS (m/z) (%) = 677.2 (100%) [M-Cl]<sup>+</sup>. IR (KBr, cm<sup>-1</sup>): 3104 ν(C-H)<sub>ar</sub>, 2921, 2856 ν(C-H)<sub>al</sub>, 1555 (ν(C=C), ν(C=N))<sub>ar</sub>, 1422 (δ(C=C), δ(C=N))<sub>ar</sub>, 1110 ν(C-O-C)<sub>as</sub>, 783 δ(C-H)<sub>oop</sub>. (Polyethylene, cm<sup>-1</sup>): 481 ν(Pd-N), 346 ν(Pd-Cl). <sup>1</sup>H NMR (CDCl<sub>3</sub> solution, 250 MHz) δ: 7.13 (s, 3H, Ph), 5.91, 5.88 (2s, 3H, CH(pz)), 4.99 (t, 4H, <sup>3</sup>J = 5.9 Hz, N<sub>pz</sub>CH<sub>2</sub>CH<sub>2</sub>O), 4.87 (t, 2H, <sup>3</sup>J = 5.9 Hz, N<sub>pz</sub>CH<sub>2</sub>CH<sub>2</sub>O), 4.60 (s, 2H, OCH<sub>2</sub>Ph), 4.37 (s, 4H, OCH<sub>2</sub>Ph), 4.31 (t, 4H, <sup>3</sup>J = 5.9 Hz, N<sub>pz</sub>CH<sub>2</sub>CH<sub>2</sub>O), 3.85 (t, 2H, <sup>3</sup>J = 5.9 Hz, N<sub>pz</sub>CH<sub>2</sub>CH<sub>2</sub>O), 2.91 (s, 9H, CH<sub>3</sub>(pz)), 2.34 (s, 9H, CH<sub>3</sub>(pz)) ppm. <sup>13</sup>C {<sup>1</sup>H} NMR (CD<sub>3</sub>CN solution, 63 MHz) δ: 150.6 (pz-C), 144.3 (pz-C), 138.6-126.2 (Ph), 107.9 (CH(pz)), 73.4 (OCH<sub>2</sub>Ph), 69.0 (N<sub>pz</sub>CH<sub>2</sub>CH<sub>2</sub>O), 49.8 (N<sub>pz</sub>CH<sub>2</sub>CH<sub>2</sub>O), 15.3 (CH<sub>3</sub>(pz)), 12.4 (CH<sub>3</sub>(pz)) ppm.

**6B.** Yield: 89% (0.171 g). C<sub>60</sub>H<sub>84</sub>Cl<sub>4</sub>N<sub>12</sub>O<sub>6</sub>Pd<sub>2</sub>: Anal. Calc.: C, 50.61; H, 5.95; N, 11.80; Found: C, 50.85; H, 5.96; N, 11.97. Conductivity (S cm<sup>2</sup> mol<sup>-1</sup>, 1.13 10<sup>-3</sup> M in CH<sub>3</sub>CN): 21.2. MS (m/z) (%) = 1389.4 (100%) [M-Cl]<sup>+</sup>. IR (KBr, cm<sup>-1</sup>): 3118 ν(C-H)<sub>ar</sub>, 2924, 2859 ν(C-H)<sub>al</sub>, 1555 (ν(C=C), ν(C=N))<sub>ar</sub>, 1450 (δ(C=C), δ(C=N))<sub>ar</sub>, 1108 ν(C-O-C)<sub>as</sub>,

824  $\delta(\text{C-H})_{\text{oop}}$ . (Polyethylene,  $\text{cm}^{-1}$ ): 492  $\nu(\text{Pd-N})$ , 365  $\nu(\text{Pd-Cl})$ .  $^1\text{H}$  NMR ( $\text{CDCl}_3$  solution, 250 MHz)  $\delta$ : 6.98 (m, 6H, Ph), 5.97 (m, 6H,  $\text{CH}(\text{pz})$ ), 4.82 (m, 12H,  $\text{N}_{\text{pz}}\text{CH}_2\text{CH}_2\text{O}$ ), 4.42 (m, 12H,  $\text{OCH}_2\text{Ph}$ ), 4.37 (m, 12H,  $\text{N}_{\text{pz}}\text{CH}_2\text{CH}_2\text{O}$ ), 2.78 (m, 18H,  $\text{CH}_3(\text{pz})$ ), 2.33 (m, 18H,  $\text{CH}_3(\text{pz})$ ) ppm.  $^{13}\text{C}\{^1\text{H}\}$  NMR ( $\text{CD}_3\text{CN}$  solution, 63 MHz,)  $\delta$ : 150.8 (pz-C), 146.1 (pz-C), 139.5-126.5 (Ph), 108.6 ( $\text{CH}(\text{pz})$ ), 73.6 ( $\text{OCH}_2\text{Ph}$ ), 69.5 ( $\text{N}_{\text{pz}}\text{CH}_2\text{CH}_2\text{O}$ ), 50.5 ( $\text{N}_{\text{pz}}\text{CH}_2\text{CH}_2\text{O}$ ), 15.1 ( $\text{CH}_3(\text{pz})$ ), 12.2 ( $\text{CH}_3(\text{pz})$ ) ppm.

#### 4 Synthesis of Pd/ $L_n$ nanoparticles

The procedure for the preparation of palladium nanoparticles is hereafter illustrated through the case of sample  $[\text{L5}]/[\text{Pd}]=0.2$  (Table 1, entry 19, Figure 3c). The procedure was similar for all other samples.

150 mg of  $[\text{Pd}_2(\text{dba})_3]$  (0.16 mmol) and the chosen quantity of **L5** (30.1 mg for  $[\text{L5}]/[\text{Pd}]=0.2$ ) were dissolved in a Fischer–Porter reactor in THF (150 mL) under argon and vigorous stirring at 196 K. The mixture was then pressurized under 3 bar of dihydrogen and left to room temperature. The color of the solution turned after 1 hour from purple to black. The hydrogen pressure and the temperature were maintained for 20 h. After that period of time, the colloidal solution is black and homogeneous. The hydrogen was evacuated and a drop of the crude colloidal solution was deposited under argon on a holey carbon covered copper grid using a paper filter under the grid for TEM and SEM analysis. Then, the colloidal solution was concentrated to *ca.* 5 ml. Addition of cold pentane (20 ml) allowed the precipitation of the particles as a black solid which was washed with pentane (3 x 20 ml) and dried under reduced pressure. The filtrated pentane from NPs precipitation was slightly yellow, showing dba elimination. This was corroborated by  $^1\text{H}$ -NMR experiments of the dried pentane solution.

## Acknowledgements

This work has been supported by the *Acción Integrada Hispano-Francesa* HF2007-0035 and the project CTQ2007-63913 BQU by the *Ministerio de Educación y Cultura* of Spain. M. Guerrero also acknowledges the *Generalitat de Catalunya* for his FI-2007 pre-doctoral grant. The authors would like to thank the Microscopy Service of the *Universitat Autònoma de Barcelona* for its technical assistance with TEM, HR-TEM and SEM. CNRS is also thanked through the LTPMM-LEA 368 action as well as Y. Coppel at the NMR service of the LCC for NMR DOSY experiments.

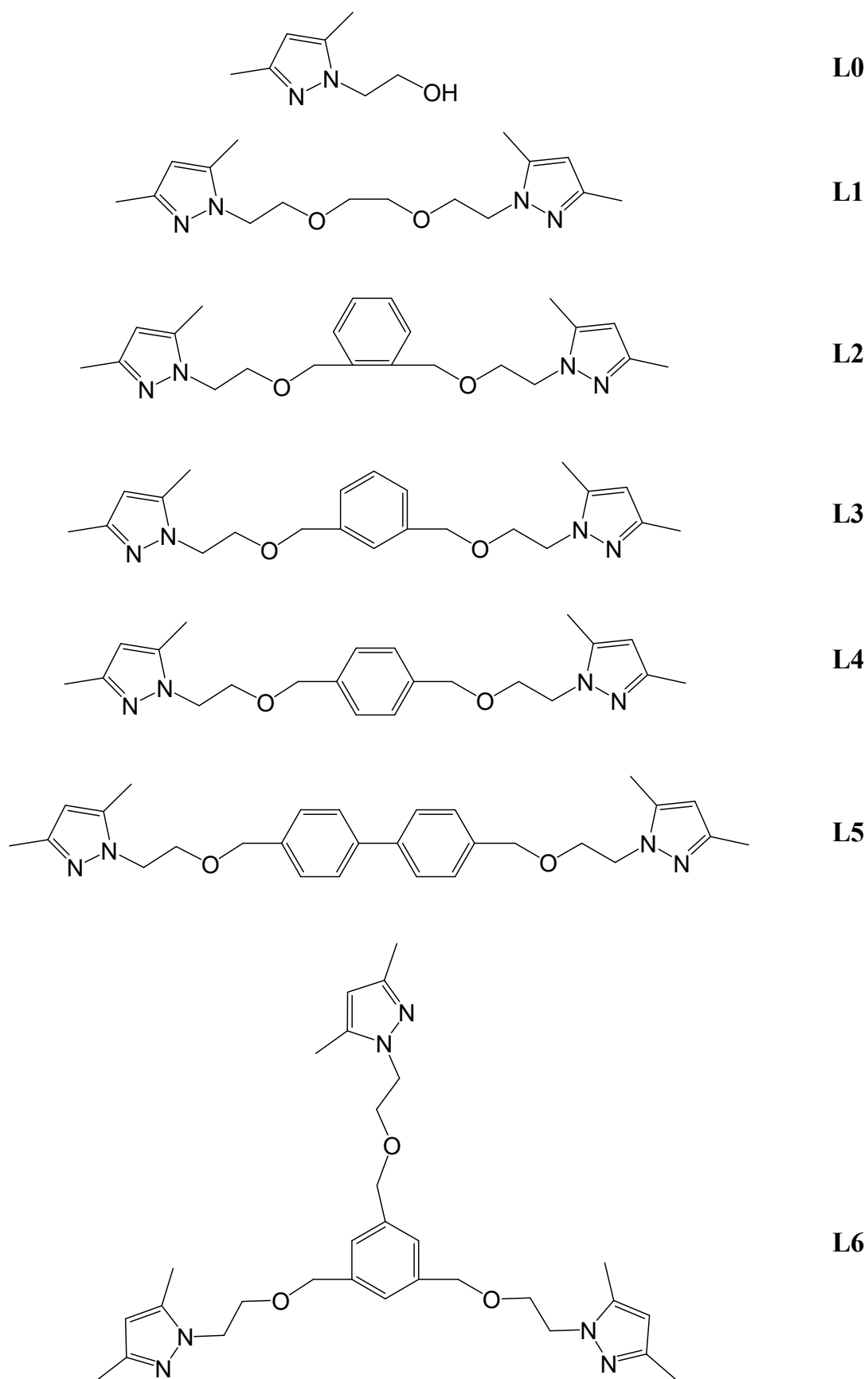
**Supporting Information Available:** Dynamic Light Scattering (DLS) measurements of  $[L2]/[Pd] = 0.5$  and  $[L5]/[Pd] = 0.2$ . This material is available free of charge via the Internet at <http://pubs.acs.org>.

**Table 1** Stabilization of palladium nanoparticles by N,O hybrid ligands L0-L6

Entry	L	[L]/[Pd] ratio	Nanoparticles d (nm)	Superstructures D (nm)
1	L0	0.1	---	---
2	L0	5.0	---	---
3	L1	0.1	---	---
4	L1	0.2	4.2(1.1)	55(10)
5	L1	0.5	4.2(1.2)	58(12)
6	L1	1.0	4.3(0.9)	56(10)
7	L2	0.1	---	---
8	L2	0.2	4.2(1.3)	130(10)
9 <sup>a</sup>	L2	0.2	4.2(1.0)	40(7)
10	L2	0.5	3.1(0.7)	155(15)
11	L2	1.0	2.5(0.8)	110(10)
12 <sup>b</sup>	L2	1.0	2.3(0.7)	125(9)
13	L3	0.1	---	---
14	L3	1.0	---	---
15	L4	0.1	---	---
16	L4	0.5	---	---
17	L4	1.0	4.4(1.2)	---
18	L5	0.1	---	---
19	L5	0.2	2.7(0.8)	120(20)
20 <sup>a</sup>	L5	0.2	2.8(0.7)	100(10)
21 <sup>b</sup>	L5	0.2	2.7(0.6)	80(10)
22 <sup>c</sup>	L5	0.2	2.8(0.9)	110(10)
23 <sup>d</sup>	L5	0.2	2.6(0.6)	120(15)
24	L5	0.5	2.6(0.7)	160(10)
25	L5	1.0	2.8(0.7)	layer
26	L5	5.0	2.4(0.8)	layer
27	L6	0.1	4.2(0.7)	layer
28	L6	0.2	4.0(0.9)	layer
29	L6	0.5	3.0(0.8)	layer
30	L6	1.0	2.6(0.8)	layer

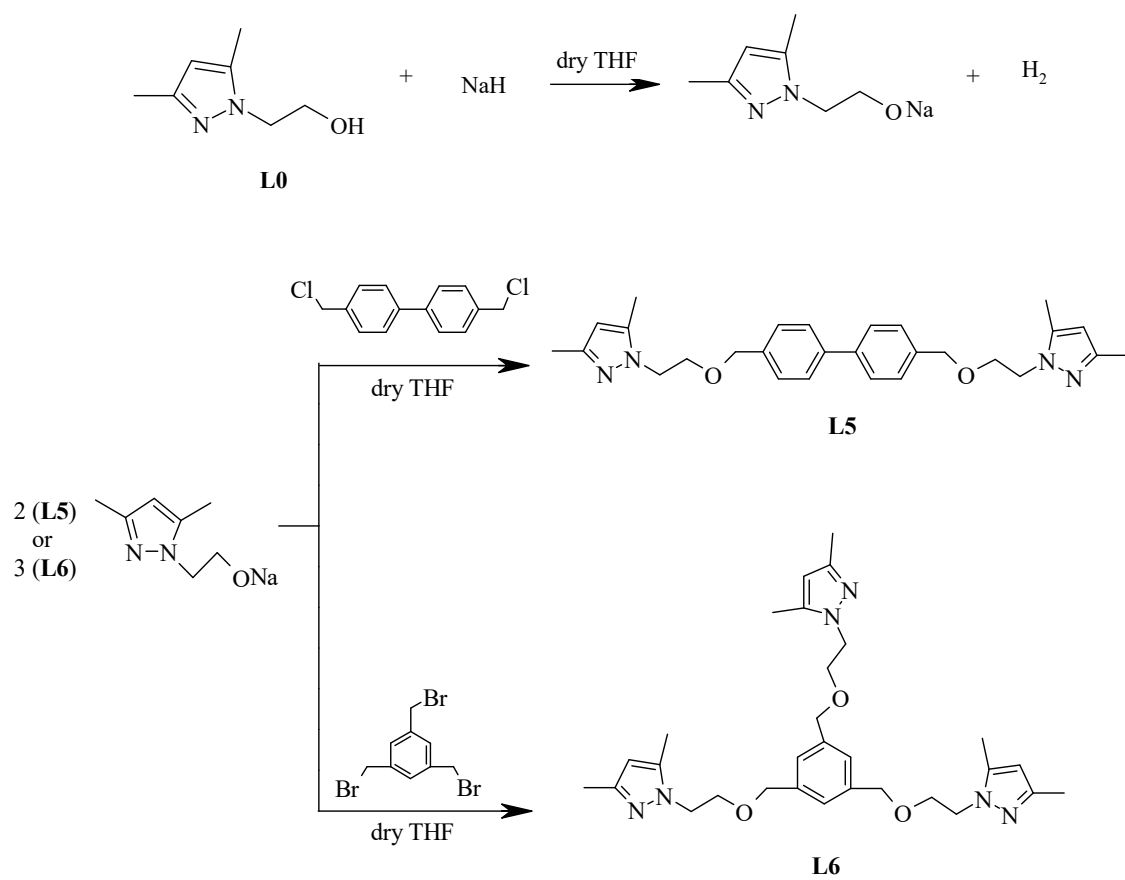
Experimental conditions: 1 mL of solvent / mg of organometallic precursor, except <sup>a</sup> where 2 mL of solvent / mg of metallic precursor was used. THF was used as solvent, except <sup>b</sup> toluene. Time of reaction = 20 h except <sup>c</sup> 1 h and <sup>d</sup> 5 h.

**Scheme 1** Scheme of the **L0 – L6** ligands.

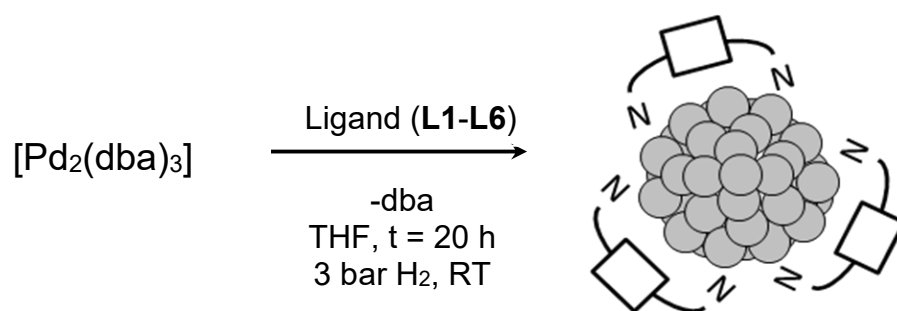




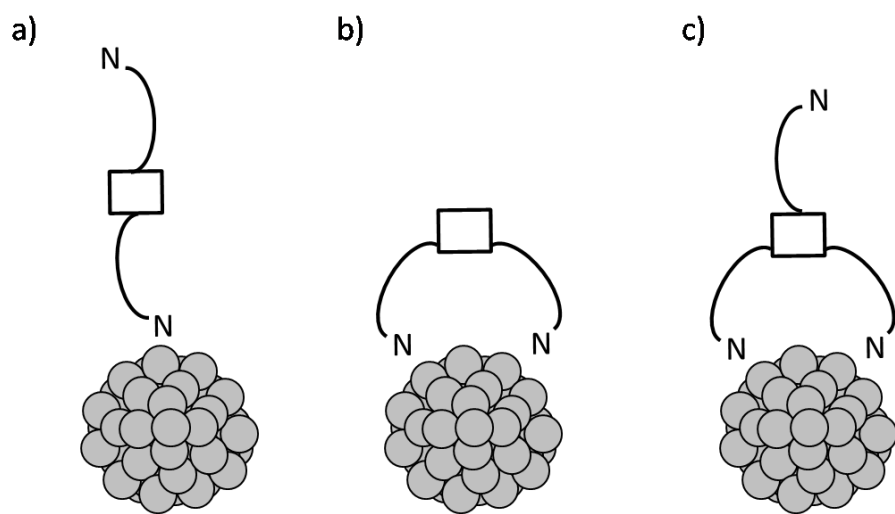
**Scheme 2** Synthesis of **L5** and **L6** ligands.



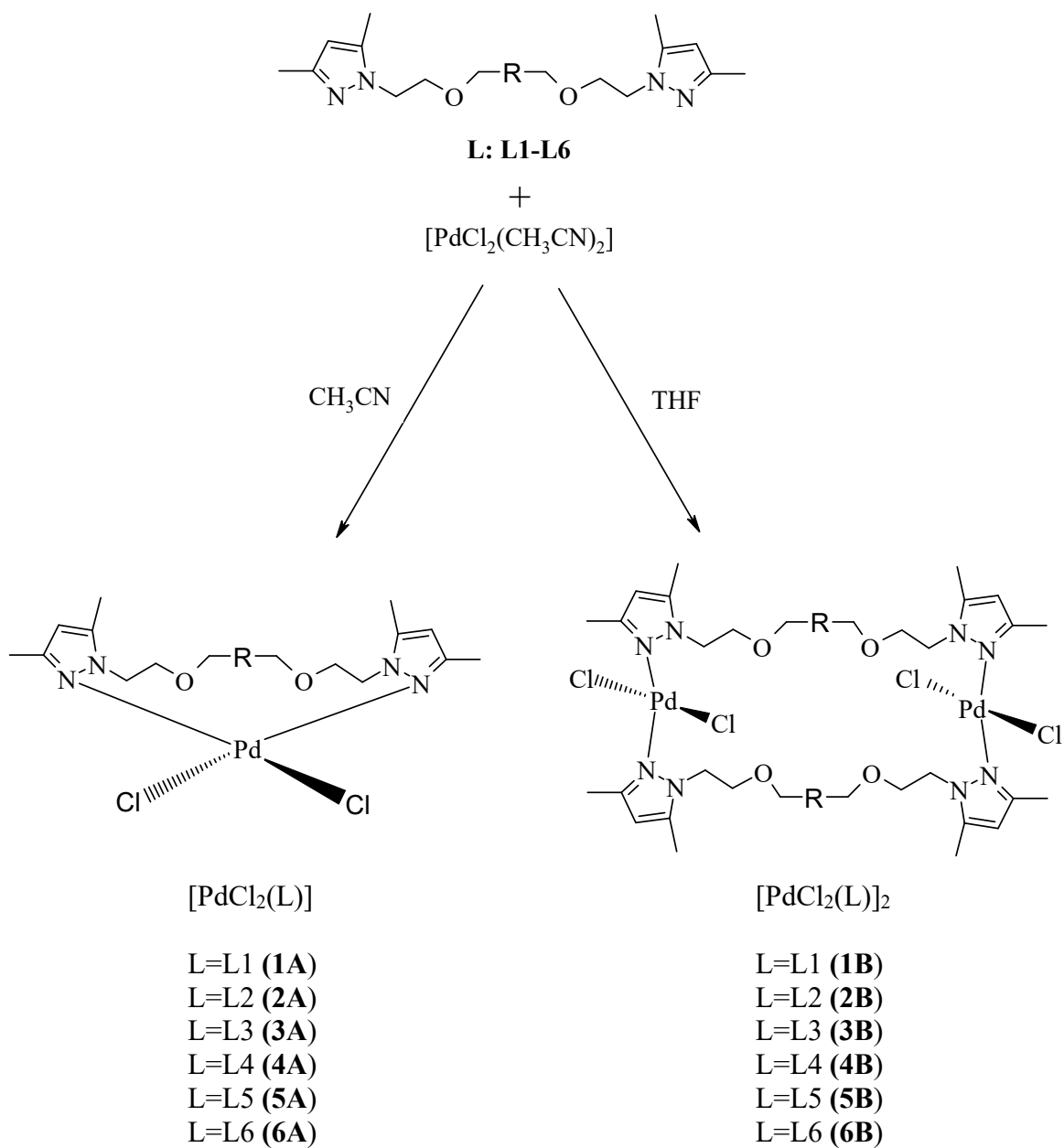
**Scheme 3** Synthesis of the Pd nanoparticles



**Scheme 4** Modes of coordination of ligands onto the surface of the nanoparticles



**Scheme 5** General synthesis of the complexes



## Figures Captions and Figures

**Figure 1** HR-TEM micrographs and the corresponding size- histograms of Pd nanoparticles synthesized as following: a) [L1]/[Pd]=0.5; b) [L2]/[Pd]=0.5; c) [L4]/[Pd]=1.0; d) [L5]/[Pd]=1.0; e) [L5]/[Pd]=5.0; f) [L6]/[Pd]=0.1 and g) [L6]/[Pd]=1.0

**Figure 2** Influence of the variation of the [L]/[Pd] ratio on the mean size of the Pd nanoparticles

**Figure 3** HR-TEM micrographs of Pd nanoparticles synthesized in THF from  $\text{Pd}_2(\text{dba})_3$  as following: a) [L1]/[Pd]=0.5; b) [L2]/[Pd]=0.5; c) [L5]/[Pd]=0.2; d) [L5]/[Pd]=5.0; e) [L6]/[Pd]=0.1 and f) [L6]/[Pd]=1.0

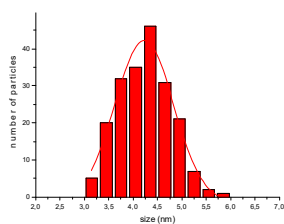
**Figure 4** SEM-FEG analyses of the Pd materials produced with a) [L5]/[Pd]=0.2 or b) [L5]/[Pd]=5.0

**Figure 5** WAXS measurements on Pd nanoparticles for [L2]/[Pd]=0.5, [L5]/[Pd]=0.2 and [L6]/[Pd]=0.2 and comparison with Pd fcc in reciprocal space (a) and real space (b).

**Figure 6** HR-TEM micrograph of Pd nanoparticles synthesized in the presence of [L5]/[Pd]=1.0 showing the interplanar spacing of (111) Pd planes (2.24 Å).

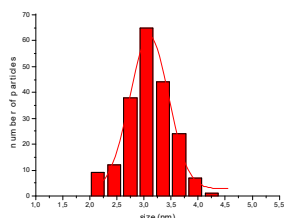
**Figure 1**

**a)**



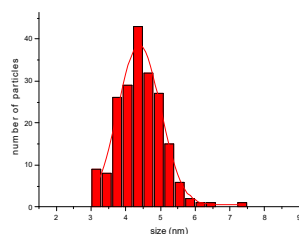
$[L1]/[Pd] = 0.5$   
 $D_{mean} = 4.2(1.2) \text{ nm}$

**b)**



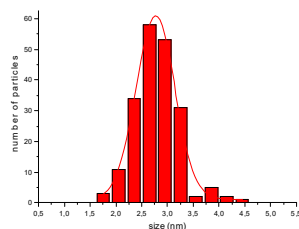
$[L2]/[Pd] = 0.5$   
 $D_{mean} = 3.1(0.7) \text{ nm}$

**c)**



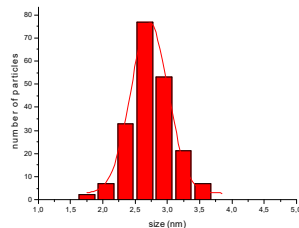
$[L4]/[Pd] = 1.0$   
 $D_{mean} = 4.4(1.2) \text{ nm}$

**d)**



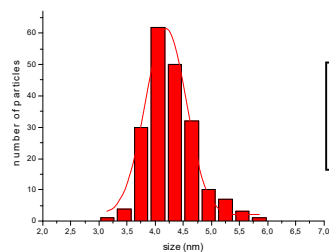
$[L5]/[Pd] = 1.0$   
 $D_{mean} = 2.8(0.7) \text{ nm}$

**e)**



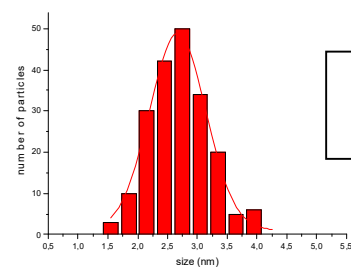
$[L5]/[Pd] = 5.0$   
 $D_{mean} = 2.4(0.8) \text{ nm}$

**f)**



$[L6]/[Pd] = 0.1$   
 $D_{mean} = 4.2(0.7) \text{ nm}$

**g)**



$[L6]/[Pd] = 1.0$   
 $D_{mean} = 2.6(0.8) \text{ nm}$

Figure 2

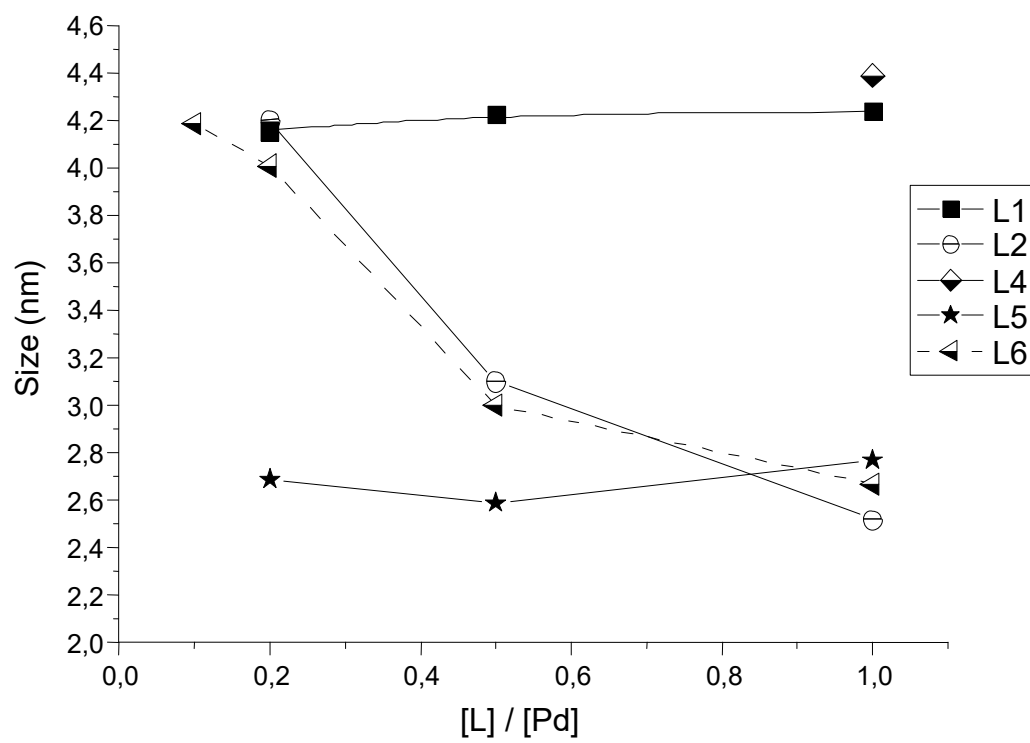


**Figure 3**

**a)**

**b)**

**c)**

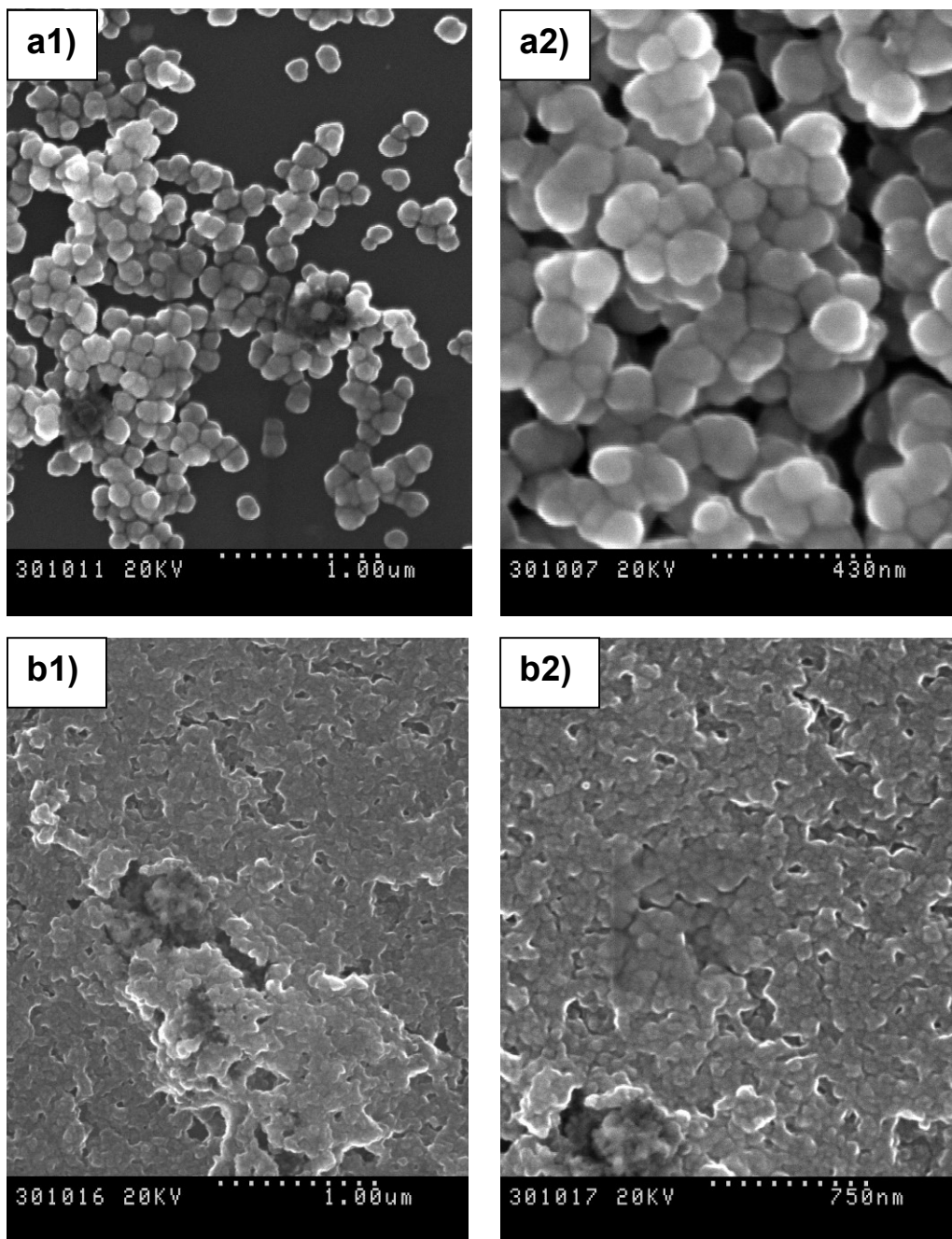
**d)**

**e)**

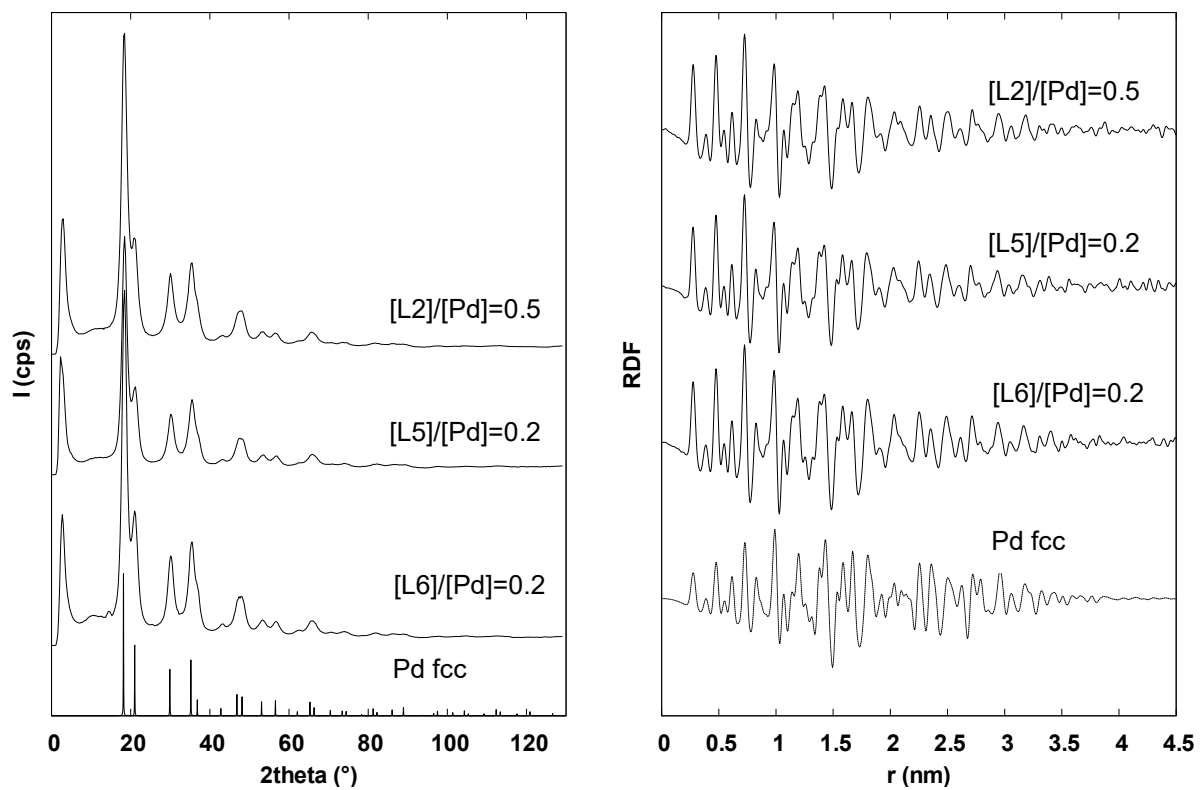
**f)**



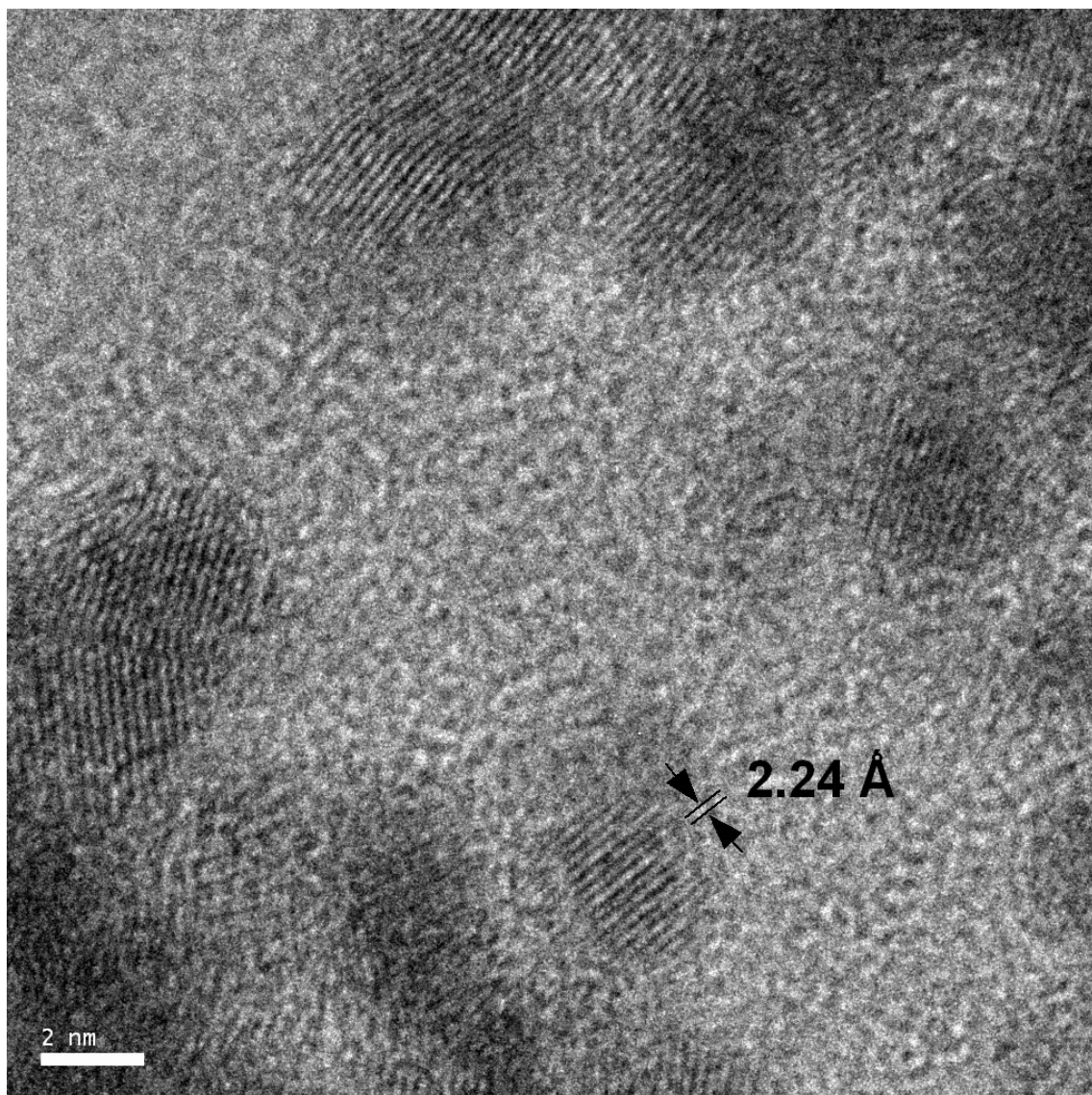
Figure 4



**Figure 5**



**Figure 6**



## References

- <sup>1</sup> Faraday, M. *Philos. Trans. Royal Soc. London* **1857**, 147, 145.
- <sup>2</sup> Tkachenko, A. G.; Xie, H.; Coleman, D.; Glomm, W.; Ryan, J.; Anderson, M. F.; Franzen, S.; Feldheim, D. L. *J. Am. Chem. Soc.* **2003**, 125, 4700.
- <sup>3</sup> Templeton, A. C.; Wuelfing, W. P.; Murray, R. W. *Acc. Chem. Res.* **2000**, 33, 27.
- <sup>4</sup> Peyser, L. A.; Vinson, A. E.; Bartko, A. P.; Dickson, R. M. *Science* **2001**, 291, 103.
- <sup>5</sup> Teng, X.; Black, D.; Watkins, N. J.; Gao, Y.; Yang, H. *Nano Lett.* **2003**, 3, 261.
- <sup>6</sup> Murphy, C. J.; Jana, N. R. *Adv. Mater.* **2002**, 14, 80.
- <sup>7</sup> Astruc, D.; Lu, F.; Aranzaes, J. R. *Angew. Chem., Int. Ed.* **2005**, 44, 7852.
- <sup>8</sup> Moreno-Mañas, M.; Pleixats, R. *Acc. Chem. Res.* **2003**, 36, 638.
- <sup>9</sup> Aiken, J. D.; Finke, R. G. *J. Mol. Catal. A: Chem.* **1999**, 145, 1.
- <sup>10</sup> Roucoux, A.; Schulz, J.; Patin, H. *Chem. Rev.* **2002**, 102, 3757.
- <sup>11</sup> Durán Pachón, L.; Rothenberg, G. *Appl. Organomet. Chem.* **2008**, 22, 288.
- <sup>12</sup> Durand, J.; Teuma, E.; Gómez, M. *Eur. J. Inorg. Chem.* **2008**, 3577.
- <sup>13</sup> Jansat, S.; Picurelli, D.; Pelzer, K.; Philippot, K.; Gómez, M.; Muller, G.; Lecante, P.; Chaudret, B. *New J. Chem.* **2006**, 30, 115.
- <sup>14</sup> Widegren, J. A.; Finke, R. G. *J. Mol. Catal. A: Chem.* **2003**, 191, 187.
- <sup>15</sup> Rao, C. N. R.; Kulkarni, G. U.; Thomas, P. J.; Edwards, P. P. *Chem. Soc. Rev.* **2000**, 29, 27.
- <sup>16</sup> Astruc, D. *Inorg. Chem.* **2007**, 46, 1884.
- <sup>17</sup> Bonnemant, H.; Richards, R. M. *Eur. J. Inorg. Chem.* **2001**, 10, 2455.
- <sup>18</sup> Martin, J.E.; Wilcoxon, J.P.; Odinek, J.; Provencio, P. *J. Phys. Chem.* **2002**, 5, 971.
- <sup>19</sup> Chen, M.; Falkner, J.; Guo, W.-H.; Zhang, J.-Y.; Sayes, C.; Colvin, V.L. *J. Colloid. Interf. Sci.* **2005**, 287, 146.
- <sup>20</sup> Schmid, G.; Harms, M.; Malm, J.; Bovin, J.; Ruitenbeck, J.; Zandbergen, H. W.; Fu, W. T. *J. Am. Chem. Soc.* **1993**, 115, 2046.
- <sup>21</sup> Reetz, M.T.; Helbig, W. *J. Am. Chem. Soc.* **1994**, 116, 7401.
- <sup>22</sup> Chen, S.; Huang, K.; Stearns, J. A. *Chem. Mater.* **2000**, 12, 540.
- <sup>23</sup> Yonezawa, T.; Imamura, K.; Kimizuka, N. *Langmuir* **2001**, 17, 4701.
- <sup>24</sup> Misukoshi, Y.; Okitsu, K.; Maeda, Y.; Yamamoto, T. A.; Oshima, R.; Nagata, Y. *J. Phys. Chem.* **1997**, B101, 7033.
- <sup>25</sup> Philippot, K.; Chaudret, K. *C. R. Chim.* **2003**, 6, 1019.
- <sup>26</sup> K. Philippot and B. Chaudret, in *Comprehensive Organometallic Chemistry* III, R.H. Crabtree & M.P. Mingos (Eds-in-Chief), Elsevier, Volume 12 – Applications III: Functional Materials, Environmental and Biological Applications, Dermot O'Hare (Volume Ed.), 2007; Chapter 12-03, 71-99.
- <sup>27</sup> Roucoux, A.; Philippot, K. *Hydrogenation With Noble Metal Nanoparticles in Handbook of Homogenous Hydrogenations*; Wiley-VCH: Weinheim, 2006.
- <sup>28</sup> Scott, R. W. J.; Ye, H.; Henriquez, R. R.; Crooks, R. M. *Chem. Mater.* **2003**, 15, 3873.
- <sup>29</sup> Ye, H.; Scott, R. W. J.; Crooks, R. M. *Langmuir* **2004**, 20, 2915.
- <sup>30</sup> Oh, S. K.; Niu, Y. H.; Crooks, R. M. *Langmuir* **2005**, 21, 10209.
- <sup>31</sup> Narayanan, R.; El-Sayed, M. A. *J. Am. Chem. Soc.* **2003**, 125, 8340.
- <sup>32</sup> Cioffi, N.; Torsi, L.; Losito, I. *Electrochim. Acta* **2001**, 46, 4205.
- <sup>33</sup> Wang, J. G.; Neoh, K. G.; Kang, E. T. *J. Colloid Interface Sci.* **2001**, 239, 78.
- <sup>34</sup> Veisz, B.; Kiraly, Z. *Langmuir* **2003**, 19, 4817.
- <sup>35</sup> Tan, H.; Zhan, T.; Fan, W.Y. *Chem. Phys. Lett.* **2006**, 428, 352.
- <sup>36</sup> Tamura, M.; Fujihara, H. *J. Am. Chem. Soc.* **2003**, 125, 15742.
- <sup>37</sup> Kim, S.-W.; Park, J.; Jang, Y.; Chung, Y.; Hwang, S.; Hyeon, T. *Nano. Lett.* **2003**, 3, 1289.
- <sup>38</sup> Schmid, G.; Maihack, V.; Lantermann, F.; Peschel, S. *J. Chem. Soc., Dalton Trans.* **1996**, 589.
- <sup>39</sup> Zelakiewicz, B. S.; Lica, G. C.; Deacon, M. L.; Tong, Y. *J. Am. Chem. Soc.* **2004**, 126, 10053.
- <sup>40</sup> Yee, C. K.; Jordan, R.; Ulman, A.; White, H.; King, A.; Rafailovich, M.; Sokolov, J. *Langmuir* **1999**, 15, 3486.
- <sup>41</sup> Ganesan, M.; Freemantle, R.G.; Obare, S.O. *Chem. Mater.* **2007**, 19, 3464.
- <sup>42</sup> Gomez, S.; Erades, L.; Philippot, K.; Chaudret, B.; Colliere, V.; Balmes, O.; Bovin, J. O. *Chem. Commun.* **2001**, 1474.
- <sup>43</sup> Pan, C.; Pelzer, K.; Philippot, K.; Chaudret, B.; Dassenoy, F.; Lecante, P.; Casanove, M. J. *J. Am. Chem. Soc.* **2001**, 123, 7584.
- <sup>44</sup> Tian, F.; Klabunde, K. J. *New J. Chem.* **1998**, 1275.

- 
- <sup>45</sup> Favier, I.; Gómez, M.; Muller, G.; Axet, R.; Castellón, S.; Claver, C.; Jansat, S.; Chaudret, B.; Philippot, K. *Adv. Synth. Catal.* **2007**, *349*, 2459 and references therein.
- <sup>46</sup> Favier, I.; Massou, S.; Teuma, E.; Gómez, M.; Philippot, K.; Chaudret, B. *Chem. Commun.* **2008**, 3296.
- <sup>47</sup> Gual, A.; Godard, C.; Philippot, K.; Chaudret, B.; Denicourt-Nowicki, A.; Roucoux, A.; Castellón, S.; Claver, C. *Chem. Sus. Chem.* **2009**, *2*, 769.
- <sup>48</sup> Guerrero, M.; Pons, J.; Branchadell, V.; Parella, T.; Solans, X.; Font-Bardia, M.; Ros, J. *Inorg. Chem.* **2008**, *47*, 11084.
- <sup>49</sup> Guerrero, M.; Pons, J.; Parella, T.; Font-Bardia, M.; Calvet, T.; Ros, J. *Inorg. Chem.* **2009**, *48*, 8736
- <sup>50</sup> Driessen, W. L.; Maase, B.; Reedijk, J.; Kooijman, H.; Lakin, M. T.; Spek, A. L. *Inorg. Chim. Acta* **2000**, *300*, 1099.
- <sup>51</sup> Driessen, W. L.; Gorter, S.; Haanstra, W. G.; Laarhoven, L. J. J.; Reeddijk, J.; Goubitz, K. F.; Seljeé, R. *Recl. Trav. Chim. Pays-Bas* **1993**, *112*, 309.
- <sup>52</sup> Pretsh, E.; Clerc, T.; Seibl, J.; Simon W. *Tables of Determination of Organic Compounds. <sup>13</sup>C NMR, <sup>1</sup>H NMR, IR, MS, UV/Vis, Chemical Laboratory Practice*; Springer-Verlag: Berlin, 1989.
- <sup>53</sup> Williams, D. H.; Fleming, I. *Spectroscopic Methods in Organic Chemistry*; McGraw-Hill: London, 1995.
- <sup>54</sup> Ramirez, E.; Jansat, S.; Philippot, K.; Lecante, P.; Gómez, M.; Masdeu, A.; Chaudret, B. *J. Organomet. Chem.* **2004**, *689*, 4601.
- <sup>55</sup> Komiya, S. *Synthesis of Organometallic Compounds: A Practice Guide*; Board: New York, 1997.